A Method for Estimation of Functional Dependence of Injection Charge Formation on Electric Field Strength

Albert Gazaryan, Andrei Sitnikov, Vladimir Chirkov, Yury Stishkov
Physics Department
St. Petersburg State University
phone: (7) 911-835-05-94
e-mail: a.gazaryan@2012.spbu.ru

***Abstract*—Improvement of EHD devices is hindered by the absence of the necessary information on the functional dependence of injection current density on the electric field strength. Investigation of the issue presents a great challenge because the quantity measured experimentally is the total current that is dependent on some almost inseparable factors. Moreover, the present theoretical dependences contradict each other and have not been verified by the experiment. In view of this, the determination of injection function is an actual problem and this paper is devoted to an attempt to solve it.**

I. Introduction

There are a number of EHD devices, basing on the injection charge formation mechanism [1], such as pumps, atomizers, heat exchangers and so on. Appropriate technologies have their unique advantages—high efficiency, durability, simple design, low acoustic noise, light weight, the rapid control of performance by varying the applied voltage, and low power consumption—over classical analogs, at least for small spatial scales [2]. However, while there are a variety of injection EHD devices, their improvement is hindered by the absence of necessary information on the functional dependence of injection current density on the electric field strength (or the so-called injection function). Investigation of the issue is a great challenge, since the quantity measured experimentally is the total current (that is dependent on some almost inseparable factors) and voltage rather than the current density and electric field strength, which actually determine the injection function. Moreover, the existing theoretical dependences [3] contradict each other and have not been verified by the experiment. Accordingly, the works of various research teams use different theoretical expressions or even autonomous injection. The most of these functions were analyzed and represented in the review article [4]. Thus, it is practically impossible at the moment to design EHD devices quantitatively due to the lack of certainty in the boundary condition for the current density. In view of this, the determination of injection function is an actual problem, and this paper is devoted to an attempt to suggest a solution.

Despite a number of disagreements in theoretical injection models [3–5], the most of researchers maintain that, for a fixed metal-liquid combination and for the isothermal liquid case, the injection function depends largely on the value of the local electric field. It thus relates the current density and the value of the local electric field at the liquid-metal interface. However, the characteristic that can be measured experimentally is the current-voltage one, whereas relationships between total current and current density as well as voltage and electric field strength are generally quite complicated and unknown. To find the electric field intensity, one has to solve the Poisson's equation and, moreover, to know the distribution of the space charge density, as it strongly affects the target value. In turn, the total current in the electrode system is governed by the superposition of the charge formation mechanisms (such as injection by the electrode and charge dissociation in the bulk) and the current passage processes. In the case of a dielectric liquid, the processes are determined by the two main components—migration and convective, the latter capable of playing a major role [6]. So, even solving the direct problem to find the total current dependence on the applied voltage by the known current density dependence on the electric field requires simulation of high-voltage current passage processes taking into account migration, but convective components of the current density (i.e., the EHD flow) and not only surface charge formation mechanism, but the space one (dissociation).

Such a method of computer simulation was developed and implemented [7, 8] relatively recently and extended later to the case of ramp voltage [9, 10]. The corresponding current-voltage characteristics (obtained at ramp voltage) in [5] were termed dynamical CVC (DCVC). Their main features that are important in the context of the present work are as follows: high speed of acquisition (both in the experiment and in the simulation), ease of repeatability testing and data collection at virtually constant external conditions [11, 12].

II. Simulation Technique

A. Mathematical Model

The computer simulation rests on the solution of the Nernst-Planck, Poisson and Navier-Stokes set of equations for isothermal incompressible liquid dielectrics [5, 13] using COMSOL Multiphysics software package:

$$div(\boldsymbol{E}) = \rho/\varepsilon\varepsilon_0 \quad (1)$$

$$\boldsymbol{E} = -\nabla\varphi \quad (2)$$

$$\partial n_i/\partial t + div(\boldsymbol{j_i}) = g(n, \boldsymbol{E}) \quad (3)$$

$$\boldsymbol{j_i} = n_i b_i \boldsymbol{E} - D_i \nabla n_i + n_i \boldsymbol{u} \quad (4)$$

$$\rho = e(n_1 - n_2) \quad (5)$$

$$\gamma\, \partial\boldsymbol{u}/\partial t + \gamma\, (\boldsymbol{u}, \nabla)\boldsymbol{u} = -\nabla P + \eta\, \Delta\boldsymbol{u} + \rho\, \boldsymbol{E} \quad (6)$$

$$div(\boldsymbol{u}) = 0 \quad (7)$$

$$g(n, \boldsymbol{E}) = \sigma_0^2/(e\,(|b_1| + |b_2|)\,\varepsilon\varepsilon_0) - e\,(|b_1| + |b_2|)/(\varepsilon\varepsilon_0)\, n_1 n_2 \quad (8)$$

where $\boldsymbol{E}$ is the electric field strength, ρ is the space charge density, φ is the electric potential, n is the ion concentration, $\boldsymbol{j}$ is the density of ion flux, σ_0 low-voltage conductivity, $\boldsymbol{u}$ is the fluid velocity, P is the pressure, ε is the relative electric permittivity, γ is the mass density, η is the dynamic viscosity, b is the ion mobility, D is the diffusion coefficient, ε_0 is the electric constant, e is the elementary electric charge, t is the time; subscript i indicates the ion species. Upon the injection of ions into a low-conducting liquid, the system has three types of ions (those injected and two dissociated species); yet, to simplify the model and to reduce the solution time, the set involves just two kinds of ions on the assumption of the similarity of properties between injected and positive dissociated ions. All ions are assumed to be monovalent.

B. Geometry and Boundary Conditions

The geometry of computer model and boundary conditions for the set of equations are presented in Fig. 1. The blade-pane electrode system was chosen for the study, as it features highly non-uniform electric field distribution needed for intensive injection charge formation and provides the stable EHD flow and total electric current (e.g., unlike the needle-plane electrode system where strong injection leads to unstable electroconvection and fluctuating total current [7]). The simulation uses a 2D model of geometry that is close to the real parameters of the experimental model, with particular emphasis on securing a good match between the shape of the injection electrode in the model and the experiment. Positive ion injection, $f_{inj}(E)$, and negative ion loss, $d_2(n_2, E)$, were set on the blade electrode, with just positive ion loss, $d_1(n_1, E)$, on the plane electrode. The charge loss is believed to be equal to the total current density for ions arriving to the boundary from the bulk:

$$d_i(n, E) = n_i b_i E_N - D_i \nabla_N n_i \tag{9}$$

where N is the surface normal. A detailed study of the simulation method can be found in [7, 8].

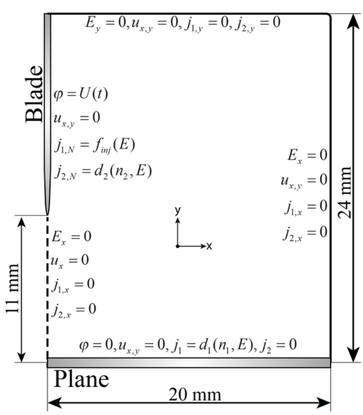

Fig. 1. Geometry of the computer model and boundary conditions.

In Fig. 1, $U(t)$ means the positive and negative ramp voltage with a ten-second period (five seconds for the rise and the drop, respectively). The test liquid in the present study was chosen to be polydimethylsiloxane-5 (PDMS-5) with the following properties: $\varepsilon = 2.4$, $\eta = 5.9\times10^{-3}$, $\gamma = 920$ kg/m^3, $\sigma_0 = 2.4\times10^{-12}$ S/m, $b = 10^{-8}$ m^2/V/s. According to the Einstein relation, the diffusion coefficient of monovalent ions is $D = 2.6\times10^{-10}$ m^2/s. However, in view of the small contribution of the diffusion component to the total flow as compared to the migration and convection cones, we use an overestimated value of the diffusion coefficient ($D = 10^{-9}$ m^2/s) in the simulation to increase the stability of the numerical solution.

C. *Method for Estimation of Injection Function*

The underlying idea for the estimation of the injection function is to select such electric-field dependence of the current density on the surface of the blade electrode that would give quantitative agreement between the integral electric current characteristics of the experiment and the simulation. The latter were taken to be DCVCs, measured and calculated over a wide voltage range. To compare the simulation and experiment correctly, the total electric current (in Amps) in calculation by the simulation results (in Amps/m) was doubled due to the reflexive symmetry and multiplied by the actual length of the experimental cell (0.06 m).

The procedure for finding the injection function consists of a number of consecutive steps. The first one is to obtain experimental DCVCs. A key requirement here is using such combination of liquid and electrode system that allows the typical injection currents to be easily detected against the background of conductivity currents.

Then, the testing injection function is introduced into the computer model, and the DCVCs are calculated on the basis of the set of Eq. (1)–(8) and the Shockley-Ramo theorem [14, 15] also known as the Sato's equation (10) [16]. The last allows finding the total electric current, which is an experimentally measurable quantity, from the current density obtained in computer simulation.

$$I = \int_V (\boldsymbol{j}, \boldsymbol{f_E}) dV, \tag{10}$$

where $\boldsymbol{f_E} = \boldsymbol{E}/\varphi_0$ is the weighting electric field, φ_0 is the applied voltage and V is the the volume.

The next step is to compare results and refine the testing function. The procedure is repeated until a match with a desired precision is attained. The step is illustrated in Fig. 2.

Finally, to verify the results by an independent parameter, which was selected to be the distribution of the EHD flow, an experimental study of the velocity field is to be done and then compared with the calculated values obtained at the last iteration.

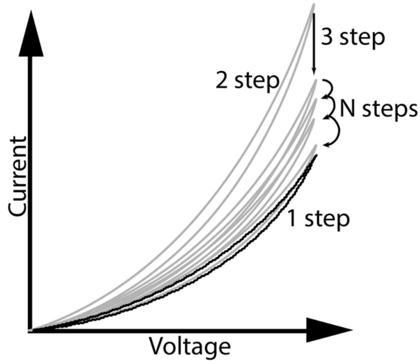

Fig. 2. Graphic illustration of the injection function estimation method by DCVC.

III. RESULTS AND DISCUSSION

A. Electric Current Characteristics

Let us consider the results. Fig. 3 shows the experimental and numerical current-voltage characteristics of the blade-plane electrode system in a wide voltage range (approximately up to 27 kV). Positive and negative ramp voltage (rise and drop segments) is applied to the system under study in an experiment using a picoammeter to measure the electric current. In the simulation, the total current was calculated by the current density (10) with the help of Sato's equation. The maximum current value attained in the system during the experiment, 300 nA, corresponds to the 27 kV and positive polarity on the blade-electrode (Fig. 3, curve 1). Upon the polarity inversion, the maximum current markedly reduces to the value of 15 nA (Fig. 3, curve 2). In view of significant nonlinearity of experimental DCVC for positive polarity and such a large difference in the current values after the polarity change, it can be concluded that the current at the positive polarity is determined by the injection. Thus, PDMS-5 and the blade-plane electrode system perform well in implementation of the injection function estimation method.

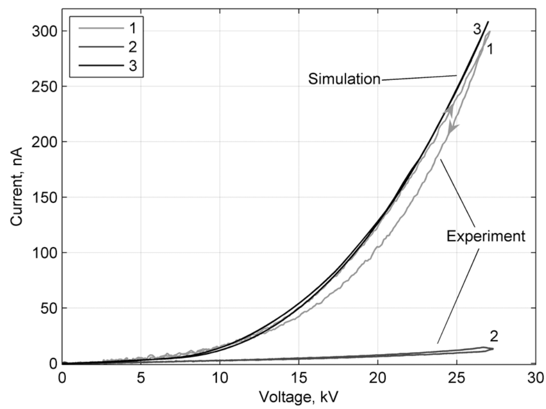

Fig. 3. Experimental DCVC for positive (curve 1) and negative (curve 2) polarity as well as DCVC obtained from the simulation (curve 3).

In Fig. 3 (curves 1 and 2), the difference between the direct and reverse branches (the so-called hysteresis) is related to the fact that the system fails to adapt to the dynamically varying voltage, and the liquid accumulate the space charge, which reduces the external electric field and thereby decreases injection from the high voltage electrode. Therefore, the downward part of the DCVC loop lies below the upward one.

Curve 3 in Fig. 3 shows the DCVC obtained at the last iteration of the above method. The estimated injection function of the following form:

$$f_{inj}(E) = A_1 E + A_2 (E - E_{st})^2 \, \theta(E - E_{st}), \qquad (11)$$

where θ is the Heaviside step function and E_{st} is the threshold value of electric field, yields a good agreement with the experimental DCVC, when $A_1 = 5.3\times10^7$ 1/(m V s), $A_2 = 0.9\times10^3$ 1/(V^2 s), and $E_{st} = 1.3\times10^7$ V/m. It describes two processes: the electrochemical reaction between the electrode metal and the liquid (the first term) and the high-voltage injection (the second term). The first process has no threshold and starts as soon as the electric field appears. The second one has a threshold and becomes active after a certain moment, when the electric field strength in the high voltage electrode exceeds the value of E_{st}. The only small difference between the calculated and experimentally obtained DCVCs is the absence of the hysteresis in the simulation. It should be noted that the injection function dependence on the electric field was selected as simple as possible (in our case, we got a set of linear and quadratic functions).

B. *Velocity Field*

Apart from the current-voltage characteristics, the velocity field of an EHD flow in the blade-plane electrode system was measured by the PIV method. The latter is commonly used in the experimental fluid dynamics [17]. It consists of seeding a flow with small tracer particles and tracking these particles to determine the velocity field of the test zone. The laser illuminates the cross-section of the system by two pulse scintillations, and at these instants, a camera records the positions of the illuminated particle. Subsequently, basing on the displacement of the particles in the two frames, commercial program DaVis restores the velocity field.

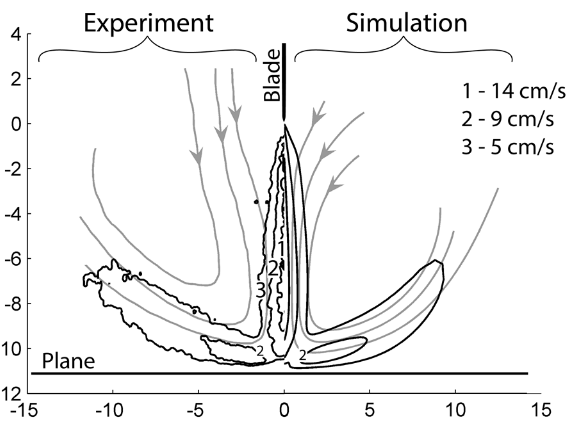

Fig. 4. Velocity field distribution in blade-plane electrode system in the case of experiment (left-hand side) and simulation (right-hand side).

The PIV experiment was held under the same conditions, when the electric current characteristics were obtained (at ramp voltage). The black lines on the left-hand side of Fig. 4 represent velocity contour lines obtained in the experiment at 13 kV. The velocity field was restored only by a single pair of frames, so the velocity contours have small fluctuations (using more pairs of frames was not possible due to the varying voltage). The contour lines with similar values (14 cm/s, 9 cm/s, and 5 cm/s) are presented on the right-hand side of Fig. 4, which corresponds to simulation, which used the estimate (11) as the injection function. Gray lines on the left- and the right-hand sides of Fig. 4 illustrate the fluid streamlines in the experiment and the simulation, respectively. The experimental and simulation contour plots can be seen to agree very well qualitatively and quantitatively (within the experimental data accuracy).

IV. Conclusion

The proposed method is a realistic way to quantify injection function. It can be used to obtain the data needed to design EHD devices, as well as to validate the existing theoretical formulas.

Despite the relatively high complexity (the combination of calculation and experiment with the restoration of the exact geometry of the electrode), simplification of the technique seems unlikely in view of the essential role of each of the factors taken into account (convection, electrode shape, conductivity and so on).

For a better match with experimental currents, the injected ions may have to be described using a single type of particles (i.e., add another Nernst-Planck equation).

Acknowledgment

Research was carried out using resources provided by the Computer Center of SPbU, Center "Geomodel" and Center for Diagnostics of Functional Materials for Medicine, Pharmacology and Nanoelectronics of Research park of St. Petersburg State University.

References

[1] J. Shrimpton, *Charge Injection Systems: Physical Principles, Experimental and Theoretical Work*, Berlin: Springer, 2009.

[2] M. R. Pearson and J. Seyed-Yagoobi, “Experimental study of EHD conduction pumping at the meso- and micro-scale,” *J. Electrostat.*, vol. 69, no. 6, pp. 479–485, 2011.

[3] A. I. Zhakin, “Near-electrode and transient processes in liquid dielectrics,” *Phys. Usp.*, vol. 49, pp. 275–295, 2006.

[4] Y. K. Suh, “Modeling and simulation of ion transport in dielectric liquids - Fundamentals and review,” *IEEE Trans. Dielectr. Electr. Insul.*, vol. 19, no. 3, pp. 831–848, 2012.

[5] Yu. K. Stishkov and A. A. Ostapenko, *Electrohydrodynamical Flows in Liquid Dielectrics,* Publishing House of Leningrad State Univ., Leningrad, 1989 (in Russian).

[6] Yu. K. Stishkov and V. A. Chirkov, “Electrohydrodynamic mechanism of the electric conduction,” in *Journal of Chemical Information and Modeling*, 2013, vol. 53, no. 9, pp. 56–61.

[7] Y. K. Stishkov and V. A. Chirkov, “Formation of electrohydrodynamic flows in strongly nonuniform electric fields for two charge-formation modes,” *Tech. Phys.*, vol. 57, no. 1, pp. 1–11, 2012.

[8] V. A. Chirkov and Y. K. Stishkov, “Current-time characteristic of the transient regime of electrohydrodynamic flow formation,” *J. Electrostat.*, vol. 71, no. 3, pp. 484–488, 2013.

[9] Y. K. Stishkov, V. A. Chirkov, and A. A. Sitnikov, “Dynamic current-voltage characteristics of weakly conducting liquids in highly non-uniform electric fields,” *Surf. Eng. Appl. Electrochem.*, vol. 50, no. 2, pp. 135–140, 2014.

[10] V. A. Chirkov, Y. K. Stishkov, and A. A. Sitnikov, “Simulation of the integral electric current characteristics of unsteady-state current passage through liquid dielectrics,” *IEEE Trans. Dielectr. Electr. Insul.*, vol. 22, no. 5, pp. 2763–2769, 2015.

[11] V. A. Chirkov, A. A. Sitnikov, and Y. K. Stishkov, “A technique for rapid diagnostics of dielectric liquids basing on their high-voltage conductivity,” *J. Electrostat.*, vol. 81, pp. 48–53, 2016.

[12] V. A. Chirkov, Yu. K. Stishkov, A. A. Sitnikov, "Features of current passage processes in liquid dielectrics at the injection and dissociation mechanisms of charge formation," *Int. J. Plasma Environ. Sci. Technol.*, vol. 10, pp. 6–10, 2016.

[13] A. Castellanos, *Electrohydrodynamics*, Wien: Springer, 1998.

[14] W. Shockley, “Currents to Conductors by a Moving Point Charge,” *J. Appl. Phys.*, vol. 9, no. 1, pp. 635–636, 1938.
[15] S. Ramo, “Currents Induced by Electron Motion,” *Proc. Inst. Radio Eng.*, vol. 27, no. 9, pp. 584–585, 1939.
[16] N. Sato, “Discharge current induced by the motion of charged particles,” *J. Phys. D Appl. Phys.*, vol. 13, pp. 3–7, 1980.
[17] P. Traoré, M. Daaboul, and C. Louste, “Numerical simulation and PIV experimental analysis of electrohydrodynamic plumes induced by a blade electrode,” *J. Phys. D. Appl. Phys.*, vol. 43, pp. 1–8, 2010.